Temperature-induced sign change of the magnetic interlayer coupling in Ni/$Ni_{25}Mn_{75}$/Ni trilayers on Cu_3Au(001)

Y. A. Shokr,[1] M. Erkovan,[2] C.-B. Wu (吴啟彬),[3] B. Zhang (张彬),[1] O. Sandig,[1] and W. Kuch[1]
[1]*Institut für Experimentalphysik, Freie Universität Berlin, Arnimallee 14, 14195 Berlin, Germany*
[2]*Nanoscience and Nanoengineering Department, Sakarya University, 54687 Sakarya, Turkey*
[3]*Department of Physics, Chung Yuan Christian University, Chungli 32023, Taiwan*

(Received 20 January 2015; accepted 20 April 2015; published online 4 May 2015)

We investigated the magnetic interlayer coupling between two ferromagnetic (FM) Ni layers through an antiferromagnetic (AFM) $Ni_{25}Mn_{75}$ layer and the influence of this coupling on the exchange bias phenomenon. The interlayer coupling energy of an epitaxial trilayer of 14 atomic monolayers (ML) Ni/45 ML $Ni_{25}Mn_{75}$/16 ML Ni on Cu_3Au(001) was extracted from minor-loop magnetization measurements using *in-situ* magneto-optical Kerr effect. The interlayer coupling changes from ferromagnetic to antiferromagnetic when the temperature is increased above 300 K. This sign change is interpreted as the result of the competition between an antiparallel Ruderman-Kittel-Kasuya-Yosida (RKKY)-type interlayer coupling, which dominates at high temperature, and a stronger direct exchange coupling across the AFM layer, which is present only below the Néel temperature of the AFM layer. © *2015 AIP Publishing LLC*. [http://dx.doi.org/10.1063/1.4919597]

INTRODUCTION

The interlayer exchange coupling between magnetic ultrathin films across a spacer material has an important influence on the magnetization reversal in multilayered structures, and thus on their magneto-resistive properties. Understanding and control of this coupling is important for many technological applications[1,2] like two[3] and three[4] dimensional magnetic ratchet memories, controllable transport of magnetic beads,[5] and mass memories.[6] All of these applications consist of several ferromagnetic and nonmagnetic or antiferromagnetic layers. While in the case of nonmagnetic spacer layers, the interlayer coupling strength depends mainly on the spacer layer thickness,[7] for antiferromagnetic spacer layers, the interlayer coupling will also depend on the magnetic state of the antiferromagnetic material, possibly influenced by proximity effects.[8]

We show here that variation of temperature can induce a change of the sign of the magnetic interlayer coupling. Since the interlayer coupling is important for the response of spin-valve devices to an external magnetic field, the ability to control the coupling direction after the preparation might provide new possibilities for applications of such spin-valve structures. The total interlayer coupling results from a competition[9] between (1) direct ferromagnetic coupling through pinholes,[10,11] (2) magnetostatic interactions like orange peel coupling originating from the presence of magnetic charges on rough interfaces,[12,13] coupling by stray field due to magnetic domain structures[14,15] or from the sample edges in small-sized structures,[16] (3) Ruderman-Kittel-Kasuya-Yosida (RKKY) coupling from the correlation energy between two FM layers through the conduction electrons of the spacer layer,[17–19] and in the case of an antiferromagnetic spacer material, (4) direct exchange interaction mediated by the antiferromagnetic exchange interaction within the AFM spacer layer.[20–22] These interaction mechanisms are active both in in-plane- and out-of-plane-magnetized films, while their relative strength may vary. Numerous theoretical and experimental investigations of the different interlayer coupling mechanisms are found in literature.[10–22]

Experimentally, the separation of these contributions is not straightforward. Often different samples with different spacer layer thicknesses are prepared for that purpose. The measurement of partial magnetization loops yields information about the presence of different species in a sample and their interaction.[23,24] In the simpler case of a magnetic trilayer with clearly distinguishable coercivities of the two ferromagnetic layers, a minor-loop measurement is sufficient to extract information about the interlayer coupling.

In this article, the temperature dependence of the magnetic interlayer coupling across an AFM spacer layer is investigated by measuring minor loops using magneto-optical Kerr effect (MOKE). Ni_xMn_{1-x} was chosen as AFM, since it has one of the highest antiferromagnetic ordering temperatures (T_{AFM}), which makes it suitable for use at elevated temperatures in practical devices. Ni was used for the FM layers, where the thickness was adjusted to have out-of-plane magnetization on a Cu_3Au(001) single crystal substrate.[25,26] x was chosen around 25%, since at this concentration, Ni_xMn_{1-x} exhibits the maximum exchange bias (EB).[27] At a thickness of 45 atomic monolayers (ML), the antiferromagnetic ordering temperature of $Ni_{25}Mn_{75}$ is around room temperature (RT, $T_{AFM} = 340$ K), and thus lower than the ordering temperature of the Ni FM layer, which is around 460 K at the chosen thicknesses of 14–16 ML.[28] This spacer-layer thickness has been chosen since clear two-step loops could be observed up to a temperature higher than T_{AFM}, such that sign and strength of the coupling could be identified. Growth and structure of epitaxial $Ni_{25}Mn_{75}$ films on Cu_3Au(001) and on Ni/Cu_3Au(001) have been discussed in Refs. 25 and 26.

EXPERIMENT

All experiments have been performed *in situ* in an ultra-high vacuum chamber with a base pressure less than

3×10^{-10} mbar. The chamber is designed for both thin film preparation and *in situ* magnetic characterization. Before growth of the sample, the substrate was cleaned by Ar^+ sputtering (1–2 keV) and annealing at 800 K for 15 min. The sputtering and annealing sequence was repeated until a sharp low-energy electron diffraction (LEED) pattern was observed. Electron-beam evaporators were used for the deposition of Ni and Mn from high-purity metal rods (99.999% for Ni, 99.99% for Mn) at RT. NiMn was deposited by simultaneous evaporation of Ni and Mn. The film thickness was monitored by medium-energy electron diffraction (MEED) during growth. A typical deposition rate was 1 ML/min. Magnetic hysteresis loops of the samples were recorded by polar MOKE using a diode laser with 634 nm wavelength and a photoelastic modulator. The chemical composition of Ni_xMn_{1-x} was analyzed by Auger electron spectroscopy.

After deposition of a $Ni_{25}Mn_{75}$/Ni bilayer on Cu_3Au (001), the sample was heated to 480 K and then cooled in a magnetic field of +200 mT to 160 K. Subsequently, temperature-dependent MOKE measurements were performed while increasing the temperature from 160 K to 420 K at intervals of about 20 K. After that, the top FM layer (14 ML Ni) was evaporated at RT, and the same field-cooling and MOKE measurement procedures were performed again for the trilayer.

RESULTS AND DISCUSSION

Figure 1 shows the major loop (black line) and minor loops (red and green lines) of the trilayer, measured at 240 K. The major loop shows two steps at 107 and 250 mT. On comparison with the magnetization loop of the bilayer, we conclude that the bottom Ni layer is the harder of the two FM layers with the higher coercivity. The minor-loop measurements were acquired by saturating the harder layer to either the positive or negative field direction, and then ramping the field below the coercivity of the hard layer. The horizontal shift of the center of the minor loops away from zero field results from the combined effect of the interlayer exchange coupling J_{IEC} through the AFM layer and the exchange bias of the soft layer by the AFM layer, characterized by the exchange bias coupling energy J_{eb}. While the former changes sign when the hard layer magnetization direction is reversed, the sign of the latter is set during the field cooling and remains constant. This can be used to separate these two effects. The coupling strength J is then taken from the product of the field offset and the magnetization of the soft layer,[22] where we assign negative values to antiparallel coupling

$$J_n = \mu_0 M_{sNi} H_n \quad \text{and} \quad J_p = \mu_0 M_{sNi} H_p \tag{1}$$

with H_n and H_p as the shift field of the negative and positive minor-loops, respectively.

It is thus

$$J_n = (J_{eb} + J_{IEC}), \quad J_p = (J_{eb} - J_{IEC}), \quad \text{and so}$$
$$J_{IEC} = (J_n - J_p)/2, \quad J_{eb} = (J_n + J_p)/2. \tag{2}$$

The shift of the positive minor loop to the left with respect to the negative one indicates a ferromagnetic coupling between the two FM layers. Examples of minor loops for different temperatures are displayed in Fig. 2. At low temperatures, J_{IEC} is positive. With increasing temperature the coercivity decreases, as well as the loop shift, and eventually J_{IEC} reverses sign at higher temperatures. The resulting J_{IEC} as a function of temperature is calculated by using Eq. (2) and shown in Fig. 3. It is observed that the interlayer coupling changes sign at about 325 K, corresponding to a change of the coupling from FM to AFM. The AFM coupling at higher temperatures can be also observed in the major loops. One example is shown in the inset of Fig. 3, where the reduced remanence of the hysteresis loop at 380 K indicates that the two FM layers are AFM-coupled.

J_{IEC} is the sum of direct exchange coupling (J_d) by the spin structure of the AFM layer and indirect coupling between the two FM layers through the AFM layer. The latter can be

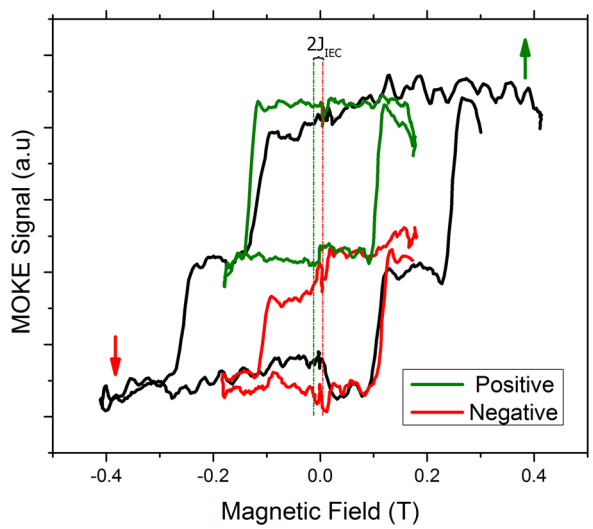

FIG. 1. Major magnetization loop (black) as well as positive (green) and negative (red) minor loops of 14 ML Ni/45 ML $Ni_{25}Mn_{75}$/16 ML Ni at 240 K. The green (red) curve was taken while the hard layer was saturated in positive (negative) field direction.

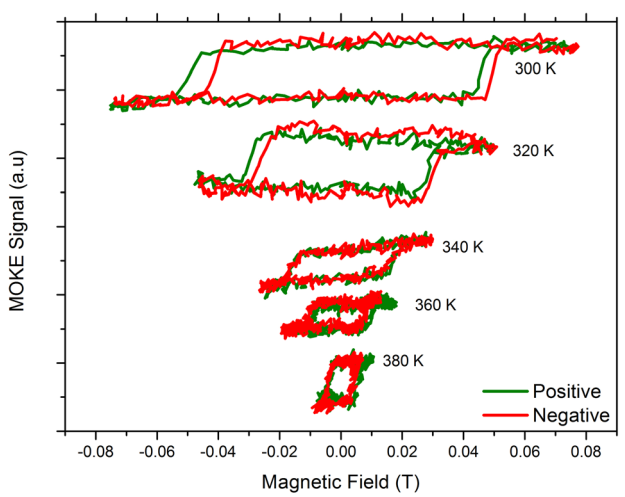

FIG. 2. Minor-loop measurements of 14 ML Ni/45 ML $Ni_{25}Mn_{75}$/16 ML Ni at different temperatures. The color code is the same as in Fig. 1.

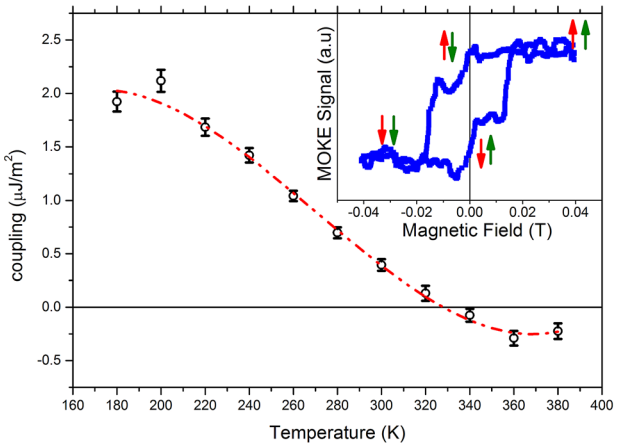

FIG. 3. Temperature dependence of the interlayer coupling between the top and the bottom Ni layer in 14 ML Ni/45 ML $Ni_{25}Mn_{75}$/16 ML Ni. The dashed line is a guide to the eye. The inset shows the major hysteresis loop measured at 380 K. The remanence less than saturation indicates that the two Ni layers are antiferromagnetically coupled.

due either to magnetostatic coupling J_{Neel} and/or the RKKY interaction, J_{RKKY},

$$J_{\mathrm{IEC}} = J_{\mathrm{d}} + J_{\mathrm{Neel}} + J_{\mathrm{RKKY}}. \tag{3}$$

J_{Neel}, J_{d}, as well as J_{RKKY} do not change sign as a function of temperature.[29] This means that the observed sign change must come from different temperature dependencies of the different contributions. The direct exchange coupling is strongly temperature-dependent around the ordering temperature of the AFM, where this coupling contribution vanishes, while the RKKY and magnetostatic coupling exhibit a more gradual temperature dependence.[30] We thus suggest that the direct exchange coupling, which is positive at that particular thickness of the $Ni_{25}Mn_{75}$ layer, dominates the coupling below the antiferromagnetic ordering temperature, while indirect coupling, RKKY and magnetostatic coupling, are dominating at temperatures higher than 340 K. The value of the AFM coupling energy at 380 K is about $-0.25\ \mu\mathrm{J/m^2}$. This value is within the range expected for RKKY-type coupling at a spacer-layer thickness of 45 ML, using typical values of similar systems[24,31,32] and extrapolating to the ninth antiferromagnetic coupling maximum using the formula of Ref. 32, assuming a decay length to account for nonzero sample temperature of 10 Å. RKKY coupling alone could thus be responsible for the observed antiferromagnetic coupling.

Finally, the temperature dependences of the coercivity H_{C} and the EB field H_{eb} of the bilayer and the trilayer are presented in Fig. 4. The temperature at which H_{C} deviates from the weak linear dependence on temperature at higher temperatures is considered the ordering temperature of the AFM, T_{AFM},[26,27] and the temperature where EB vanishes is taken as blocking temperature (T_{b}). T_{AFM} and T_{b} for the trilayer sample are (360 ± 15) and (260 ± 15) K, respectively.

T_{AFM} of the trilayer as extracted from the temperature dependence of H_{C} is around 360 K, which confirms the assumption of the disappearance of direct exchange coupling at around this temperature. The temperature-dependent

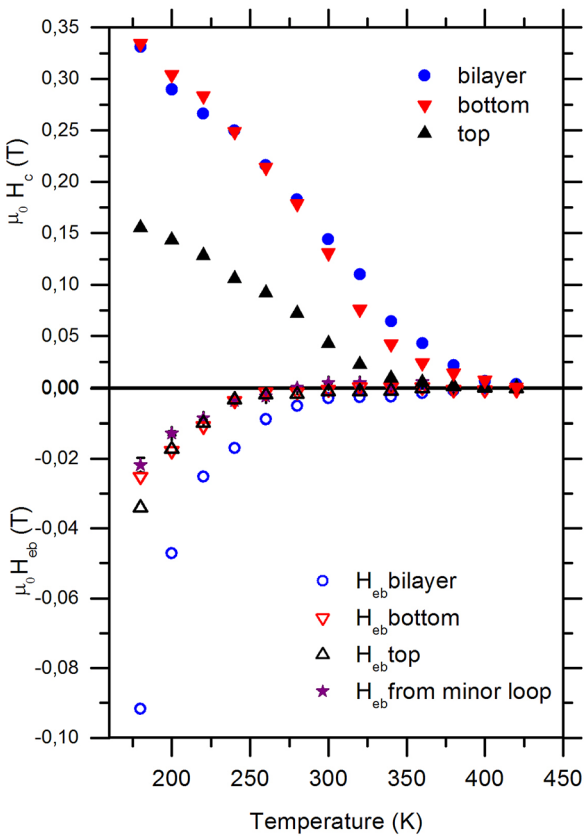

FIG. 4. Temperature dependence of the coercivity H_{C} (solid symbols) and bias field H_{eb} (open symbols) of the 45 ML $Ni_{25}Mn_{75}$/16 ML Ni bilayer (circles) and 14 ML Ni/45 ML $Ni_{25}Mn_{75}$/16 ML Ni trilayer (up- and down-triangles for top and bottom layers, respectively). Stars represent the bias field extracted from the minor loops.

exchange bias field of the top layer extracted from the minor-loop measurements (stars in Fig. 4) agrees well with the loop shift of the soft layer extracted from the major loops.

CONCLUSION

The conclusion from the presented data is that the magnetic interlayer coupling in this system is a competition between direct exchange coupling through the AFM layer favoring parallel alignment and an antiparallel RKKY-type coupling. The latter dominates at high temperatures, leading to an effective antiparallel coupling between the two Ni layers, while the direct exchange coupling is present at temperatures below the Néel temperature of the AFM layer, where it prevails over the RKKY coupling. The coupling strength at temperatures above the ordering temperature of the AFM layer is in the range of possible RKKY-type coupling energies. These competing interlayer interactions allow tuning the magnitude as well as the sign of the total interlayer coupling by variation of temperature. An AFM material with a suitable ordering temperature could therefore not only serve to enhance the temperature dependence of the coercivity of an adjacent FM layer but also to modulate the interlayer coupling and thus the remanence of a trilayer by temperature.

[1]H. W. Fuller and D. L. Sullivan, J. Appl. Phys. **33**, 1063 (1962).
[2]M. Matczak, P. Kuświk, B. Szymański, M. Urbaniak, M. Schmidt, J. Aleksiejew, F. Stobiecki, and A. Ehresmann, Appl. Phys. Lett. **100**, 162402 (2012).
[3]J. H. Franken, H. J. M. Swagten, and B. Koopmans, Nat. Nanotechnol. **7**, 499 (2012).
[4]R. Lavrijsen, J. H. Lee, A. Fernández-Pacheco, D. C. C. Petit, R. Mansell, and R. P. Cowburn, Nature **493**, 647 (2013).
[5]P. Tierno, S. V. Reddy, J. Yuan, T. H. Johansen, and T. M. Fischer, J. Phys. Chem. B **111**, 13479 (2007).
[6]H. J. Richter, J. Phys. D: Appl. Phys. **40**, R149 (2007).
[7]J. A. C. Bland and B. Heinrich, *Ultrathin Magnetic Structures* (Springer, Berlin, New York, 1994).
[8]K. Lenz, S. Zander, and W. Kuch, Phys. Rev. Lett. **98**, 237201 (2007).
[9]M. Matczak, B. Szymański, M. Urbaniak, M. Nowicki, H. Głowiński, P. Kuświk, M. Schmidt, J. Aleksiejew, J. Dubowik, and F. Stobiecki, J. Appl. Phys. **114**, 093911 (2013).
[10]J. Bobo, H. Kikuchi, O. Redon, E. Snoeck, M. Piecuch, and R. White, Phys. Rev. B **60**, 4131 (1999).
[11]D. E. Bürgler, M. Buchmeier, S. Cramm, S. Eisebitt, R. R. Gareev, P. Grünberg, C. L. Jia, L. L. Pohlmann, R. Schreiber, M. Siege, Y. L. Qin, and A. Zimina, J. Phys.: Condens. Matter **15**, S443 (2003).
[12]J. Moritz, F. Garcia, J. C. Toussaint, B. Dieny, and J. P. Nozières, Europhys. Lett. **65**, 123 (2004).
[13]L. Thomas, M. G. Samant, and S. S. P. Parkin, Phys. Rev. Lett. **84**, 1816 (2000).
[14]W. Kuch, L. I. Chelaru, K. Fukumoto, F. Porrati, F. Offi, M. Kotsugi, and J. Kirschner, Phys. Rev. B **67**, 214403 (2003).
[15]A. Anguelouch, B. D. Schrag, G. Xiao, Y. Lu, P. L. Trouilloud, R. A. Wanner, W. J. Gallagher, and S. S. P. Parkin, Appl. Phys. Lett. **76**, 622 (2000).
[16]V. Baltz, B. Rodmacq, A. Bollero, J. Ferré, S. Landis, and B. Dieny, Appl. Phys. Lett. **94**, 052503 (2009).
[17]M. A. Ruderman and C. Kittel, Phys. Rev. **96**, 99 (1954).
[18]T. Kasuya, Prog. Theor. Phys. **16**, 45 (1956).
[19]K. Yosida, Phys. Rev. **106**, 893 (1957).
[20]W. Kuch, L. I. Chelaru, F. Offi, J. Wang, M. Kotsugi, and J. Kirschner, Nat. Mater. **5**, 128 (2006).
[21]J. Wu, J. Choi, A. Scholl, A. Doran, E. Arenholz, Y. Z. Wu, C. Won, C. Hwang, and Z. Q. Qiu, Phys. Rev. B **80**, 012409 (2009).
[22]B. Zhang, C.-B. Wu, and W. Kuch, J. Appl. Phys. **115**, 233915 (2014).
[23]J. Gräfe, M. Schmidt, P. Audehm, G. Schütz, and E. Goering, Rev. Sci. Instrum. **85**, 023901 (2014).
[24]M. T. Johnson, S. T. Purcell, N. W. E. McGee, R. Coehoorn, J. aan de Stegge, and W. Hoving, Phys. Rev. Lett. **68**, 2688 (1992).
[25]W. A. A. Macedo, P. L. Gastelois, M. D. Martins, W. Kuch, J. Miguel, and M. Y. Khan, Phys. Rev. B **82**, 134423 (2010).
[26]M. Erkovan, Y. A. Shokr, D. Schiestl, C.-B. Wu, and W. Kuch, J. Magn. Magn. Mater. **373**, 151 (2015).
[27]M. Y. Khan, C.-B. Wu, and W. Kuch, Phys. Rev. B **89**, 094427 (2014).
[28]M. Y. Khan, C.-B. Wu, M. Erkovan, and W. Kuch, J. Appl. Phys. **113**, 023913 (2013).
[29]S. Schwieger, J. Kienert, K. Lenz, J. Lindner, K. Baberschke, and W. Nolting, Phys. Rev. Lett. **98**, 057205 (2007).
[30]J. M. Teixeira, J. Ventura, R. Fermento, J. P. Araújo, J. B. Sousa, S. Cardoso, and P. P. Freitas, J. Appl. Phys. **103**, 07F319 (2008).
[31]P. Bruno and C. Chappert. Phys. Rev. Lett. **67**, 1602 (1991).
[32]M. D. Stiles, J. Magn. Magn. Mater. **200**, 322 (1999).